

# Electronic pathway in the photosynthetic reaction centers and some mutation of RC's

M. Pudlak<sup>1,\*</sup> and R. Pincak<sup>1,2,†</sup>

<sup>1</sup>*Institute of Experimental Physics, Slovak Academy of Sciences,  
Watsonova 47,043 53 Kosice, Slovak Republic*

<sup>2</sup>*Joint Institute for Nuclear Research, BLTP,  
141980 Dubna, Moscow region, Russia*

(Dated: November 5, 2018)

## Abstract

The reaction center of *Chloroflexus aurantiacus* and *Rhodobacter sphaeroides* mutation of RC's was investigated. To describe the kinetic of the *Chloroflexus aurantiacus* RC's we use incoherent model of electron transfer. It was shown that the asymmetry in electronic coupling must be included to explain the experiments. For the description of *Rhodobacter sphaeroides* *H(M182)L* mutation we used partially coherent as incoherent models of electron transfer. These two models are discussed with regard to the observed electron transfer kinetics. It can be concluded that partially coherent model is more adequate. We predict some new electron pathways for describing the kinetic of RC's and some mutation.

PACS numbers: 87.15.Rn, 87.10.+e, 82.20.Fd

---

\*Electronic address: pudlak@saske.sk

†Electronic address: pincak@saske.sk

## I. INTRODUCTION

Photosynthesis is a reaction in which light energy is converted into chemical energy. The primary process of photosynthesis is carried out by a pigment-protein complex embedded in the membrane, that is, RC. In photosynthetic purple bacteria, the cyclic electron transfer reaction is performed by RC and two other components: the cytochrome (Cyt)  $bc_1$  complex, and the soluble electron carrier protein. The photosynthetic reaction centers (RC) is a special pigment-protein complex, that functions as a photochemical trap. The precise details of the charge separations reactions and subsequent dark electron transport (ET) form the central question of the conversion of solar energy into the usable chemical energy of photosynthetic organism. The function of the reaction center is to convert solar energy into biochemical amenable energy. Therefore, we wish to understand which features of the reaction center are responsible for the rate constants of these reactions.

Insight into the molecular organization of the RC has been derived, initially, from spectroscopic studies and, subsequently, from the development and analysis of high-resolution crystal structures of several photosynthetic organisms. The first RC structurally resolved (3 Å) was of the purple bacterial RC from *Rhodospseudomonas viridis* [1]. This was soon followed by the elucidation of several other purple bacterial structures. Good progress is also being made toward achieving two- and three-dimensional structures of photosystem II (PSII) crystals. It is surprising that the structures of all of the different RC's show a dimeric core with a pseudo- $C_2$  axis of symmetry.

A remarkable aspect of the RC structures is the occurrence of two almost identical electron acceptor pathways arranged along the  $C_2$  axis relative to the primary charge-separating dimer (bacterio) chlorophyll (Fig. 1). This finding posed a key question: Does electron transfer involve both branches? In the purple bacterial RC, only one branch is active although the inactive branch can be forced into operation with modification of amino acid side chains on the active branch [2]. Moreover the charge-separating electron transfer reactions occur with a remarkably high quantum yield of 96%, where from two possible symmetric branches only the branch  $L$  is active in the electron transfer. This efficiency relies on the rates of the charge-separating reactions being 2-3 orders of magnitude faster than the rates of the competing reactions.

The strong asymmetry imposed on primary charge separation photo-chemistry in the pur-

ple bacterial RC results from two homologous polypeptides that function as a heterodimer. A heterodimer is also involved in the core of the RC's of PSI and PSII. However, some RC's, such as heliobacteria [3] and green sulfur bacteria [4], contain two identical homodimeric polypeptides, and electron transfer is potentially bifurcated.

Genetic sequence information has greatly improved the understanding of the origin of the RC proteins. From the sequence analysis, it became clear that the purple bacteria RC is remarkably similar to that of PSII, and PSI was also discovered to have similarity with that of the green sulfur bacteria [5]. Recent structural comparisons between PSI and PSII, for example, show a distinct structural homology, which suggests that even these two RC's likely share a common ancestor [6].

In purple bacteria, the electron rate is sensitive to the free energy difference between the excited state and the charge-separated state but not to the relative distribution of electrons over the two macrocycles of the donor. After extensive studies, the rate is now established to be critically coupled to the properties of the bacteriochlorophyll monomer that lies between the donor and bacteriopheophytin acceptor (Fig.1). The involvement of the bacteriochlorophyll monomer may give rise to multiple pathways for electron transfer [7] and can partially determine the asymmetry of the electron transfer along one branch [8]. We believe that the reason for asymmetric ET between prosthetic groups located on different polypeptides is a different molecular dynamics. Dynamics of atoms causes the change of the electrical potential fields and the conformational variations influence the mutual orientations between cofactors. Then the energy gap and overlap of electronic wave functions fluctuates as a result in the system. The net result is a different fluctuation of electronic energy levels on prosthetic groups and also a different fluctuations of the overlaps of the electronic wave functions on *L* and *M* branches. On the other hand the chain located on subunit *M* is inactive in ET and the highly asymmetric functionality, however, can be decreased by amino acid mutations or cofactor modification. We used this approach to explain the effect of individual amino acid mutation or cofactor modifications on the observed balance between the forward ET reaction on the *L*-side of the RC, the charge recombination processes, and ET to the *M*-side chromophores [9, 10, 11, 12, 13].

The theoretical models that describe the charge transfer in reaction centers using parameters with clear physical interpretations. Some of these input parameters can not be deduced from independent experimental work. The information regarding the energetic pa-

rameters, the medium reorganization energies, the high frequency modes, and electronic coupling terms can be achieved with quantum mechanical computations. But until now these parameters which characterize the reaction centers are not available. And so we use the set of parameters which fit the experiments. Several sets of parameters were used to describe a charge transfer in the RC. A set of parameters based on molecular dynamics simulations [14] corresponds to a dominance of superexchange mechanisms for the primary ET reaction in RC's. Another set of parameters [15, 16] was used to fit experimental data. This second set of parameters derives a dominant contribution from the sequential mechanism. The first set of parameters has the larger reorganization energies and the greater coupling factors. This set of parameters makes the ET rate much larger than it is found in the wild-type proteins. The possibility to find out the input parameters from theory is comparison of observed kinetics for different mutated reaction centers. The problem is that not always the impact of mutation on the input parameters is clear. In this paper we focus on the electron transfer in two RCs. First is the RCs of the green bacterium *Chloroflexus aurantiacus*. The second is the RCs of *Rhodobacter sphaeroides* *H(M182)L* mutation. It is believed that both purple bacterial RCs and RCs from *C. aurantiacus* have a similar structure [17]. We adapt in this work the set of parameters that characterized the observed L-side experimental kinetics of wild-type (WT) RCs of *Rb.sphaeroides* very well. The *Chloroflexus aurantiacus* RC's and the RCs of *Rhodobacter sphaeroides* *H(M182)L* mutation have structural similarity but charge separation kinetics are different. Both these RCs contain BPheo pigment in M-branch in the position where BChl monomer is placed in the WT reaction center. In contrast with this structural similarity, the H(M182)L mutant reveals the electron transfer through the M branch, in the *Chloroflexus aurantiacus* RC's the M-branch is inactive.

## II. THEORY

We attempt to analyze the possibility that ET asymmetry can be described by a model which assumes that there exist vibrational modes of the medium which have a sufficient time to relax to the thermal equilibrium after each ET step. We start by considering an electron transfer system in which the electron has  $N$  accessible sites, embedded in a medium. We denote by  $|j\rangle$  the state with electron localized at the  $j$ th site and  $j = 1, 2, \dots, N$ . The  $j$  and  $k$  sites are coupled by  $V_{jk}$ . The interaction of the solvent with the system depends on

the electronic states  $|j\rangle$  by  $H_j$ . The total model Hamiltonian for the system and medium is

$$H = H_0 + V, \quad (1)$$

where

$$H_0 = \sum_{j=1}^N |j\rangle [\varepsilon_j - i\Gamma_j + H_j] \langle j|, \quad (2)$$

$$V = \sum_{j,k=1}^N V_{jk} |j\rangle \langle k|, \quad j \neq k, \quad (3)$$

where  $\varepsilon_j$  is the site energy. The parameter  $\hbar/2\Gamma_j$  has a meaning of the lifetime of the electron at site  $j$  in the limit of the zero coupling parameter. It can characterize the possibility of the electron escape from the system by another channel, for instance a nonradiative internal conversion or recombination process.

The Hamiltonian describing the reservoir consisting of harmonic oscillators is

$$H_j = \sum_{\alpha} \left\{ \frac{p_{\alpha}^2}{2m_{\alpha}} + \frac{1}{2} m_{\alpha} \omega_{\alpha}^2 (x_{\alpha} - d_{j\alpha})^2 \right\}. \quad (4)$$

Here,  $m_{\alpha}$  and  $\omega_{\alpha}$  are frequency and the mass of the  $\alpha$ th oscillator, and  $d_{j\alpha}$  is the equilibrium configuration of the  $\alpha$ th oscillator when the system is in the electronic state  $|j\rangle$ . The total density matrix  $\rho(t)$  of the ET system and the medium satisfies the Liouville equation,

$$\partial_t \rho(t) = -\frac{i}{\hbar} [H\rho(t) - \rho(t)H^{\dagger}] = -iL\rho(t). \quad (5)$$

In the interacting picture,

$$\rho_I(t) = \exp\left(\frac{i}{\hbar} H_0 t\right) \rho(t) \exp\left(-\frac{i}{\hbar} H_0^{\dagger} t\right). \quad (6)$$

The Liouville equation in the interacting picture has the following form:

$$\partial_t \rho_I(t) = -\frac{i}{\hbar} [V_I(t)\rho_I(t) - \rho_I(t)V_I^{\dagger}(t)] = -iL(t)\rho_I(t), \quad (7)$$

where

$$V_I(t) = \exp\left(\frac{i}{\hbar} H_0 t\right) V \exp\left(-\frac{i}{\hbar} H_0 t\right). \quad (8)$$

Here we denote the total trace, and the partial traces over the ET system and over the medium by  $Tr$ ,  $Tr^e$ ,  $Tr^Q$ , respectively. By definition  $Tr \equiv Tr^Q Tr^e$ . The population on state  $|j\rangle$  at time  $t$  is given by

$$P_j(t) = Tr(|j\rangle\langle j|\rho(t)). \quad (9)$$

We assume that the vibrational relaxation is sufficiently rapid so that the system can relax to thermal equilibrium after each ET step. This assumption determines a choice of projector operator. The projector operator  $D$  acting on an arbitrary operator  $B$  in the Hilbert space of the total ET system and medium is defined by [18]

$$DB = \sum_{j=1}^N Tr(|j\rangle\langle j|B)\rho_j|j\rangle\langle j|, \quad (10)$$

where  $\rho_j$  is the equilibrium medium density matrix in the state  $|j\rangle$ , i.e.,

$$\rho_j = \frac{\exp(-H_j/k_B T)}{Tr^Q \exp(-H_j/k_B T)}. \quad (11)$$

Using the standard projection operator techniques [19, 20] we can derive a generalized master equation for the populations,

$$\begin{aligned} \partial_t P_j(t) = & -\frac{2\Gamma_j}{\hbar} P_j(t) - \sum_{k=1}^N \int_0^t W_{jk}(t-\tau) P_j(\tau) d\tau \\ & + \sum_{k=1}^N \int_0^t W_{kj}(t-\tau) P_k(\tau) d\tau, \quad j = 1, \dots, N, \quad j \neq k, \end{aligned} \quad (12)$$

where

$$\begin{aligned} W_{jk}(t) = & 2 \frac{|V_{jk}|^2}{\hbar^2} \text{Re} \left\{ \exp \left[ -\frac{\Gamma_j + \Gamma_k}{\hbar} t \right] \exp \left[ \frac{i(\varepsilon_j - \varepsilon_k)}{\hbar} t \right] \right. \\ & \left. \times \exp \left\{ \sum_{\alpha} \frac{E_{jk}^{\alpha}}{\hbar \omega_{\alpha}} [(\bar{n}_{\alpha} + 1)e^{-i\omega_{\alpha} t} + \bar{n}_{\alpha} e^{i\omega_{\alpha} t} - (2\bar{n}_{\alpha} + 1)] \right\} \right\}. \end{aligned} \quad (13)$$

Here,  $\bar{n}_{\alpha} = [\exp(\hbar\omega_{\alpha}/k_B T) - 1]^{-1}$  is a thermal population of the  $\alpha$ th mode and

$$E_{jk}^{\alpha} = \frac{1}{2} m_{\alpha} \omega_{\alpha}^2 (d_{j\alpha} - d_{k\alpha})^2 \quad (14)$$

is the reorganization energy of the  $\alpha$ th mode when system transfer from state  $|j\rangle$  to state  $|k\rangle$ .

### III. MODEL OF REACTION CENTER

To describe the first step of electron transfer processes in the reaction centers we have used the 5-sites kinetic model of RC.

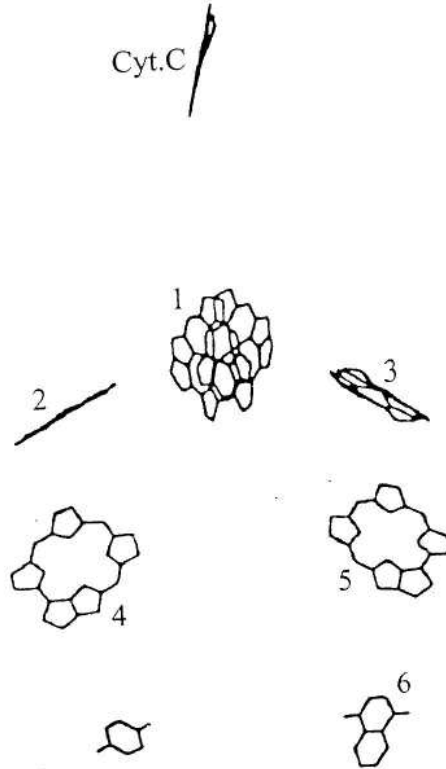


FIG. 1: The RC of purple bacteria are composed of three protein subunits called  $L$ ,  $M$  and  $H$ . Dimer  $P$  is describing by molecule 1. Cofactors in the subunits  $L$  are: 3 represent ( $BChl_L$ ) molecule 5 ( $BPh_L$ ) and 6 is ( $Q_L$ ) and identically in the subunits  $M$  ( $BChl_M$ ) is describing by molecule 2 and molecule 4 represent ( $BPh_M$ ). Cytochrom C serve as a source of electrons for reaction center.

We designate the special pair  $P$  as site 1, the sites 2 and 3 represent the molecules  $BChl_M$  and  $BChl_L$ , and the sites 4 and 5 then represent the molecules  $BPh_M$  and  $BPh_L$  (Fig. 1). We assume that we can neglect the backward electron transfer from quinone molecules and so we use the complex energies of 4,5 molecules of RC. Based on experimental observations of ET in RC, it is expected that bacteriochlorophyll play a crucial role in ET. In this 5-sites model we have assumed that ET in RC is sequential where  $P^+BChl^-$  is a real chemical intermediate. The imaginary part of energy level 1 describes the probability of electron

deactivation to the ground state. We describe the ET in the *Chloroflexus aurantiacus* RC's by the following kinetic model

$$\begin{aligned} \partial_t P_1(t) = & -\left(\frac{2\Gamma_1}{\hbar} + k_{12} + k_{13}\right)P_1(t) \\ & + k_{21}P_2(t) + k_{31}P_3(t), \end{aligned} \quad (15a)$$

$$\partial_t P_2(t) = -(k_{21} + k_{24})P_2(t) + k_{12}P_1(t) + k_{42}P_4(t), \quad (15b)$$

$$\partial_t P_3(t) = -(k_{35} + k_{31})P_3(t) + k_{13}P_1(t) + k_{53}P_5(t), \quad (15c)$$

$$\partial_t P_4(t) = -\left(\frac{2\Gamma_M}{\hbar} + k_{42}\right)P_4(t) + k_{24}P_2(t), \quad (15d)$$

$$\partial_t P_5(t) = -\left(\frac{2\Gamma_L}{\hbar} + k_{53}\right)P_5(t) + k_{35}P_3(t). \quad (15e)$$

Here we denote  $k_{ij}(s \rightarrow 0^+) = k_{ij}$  and  $k_{ij}(s \rightarrow 0^+) = \int_0^\infty W_{ij}(t)dt$ .

We assume that the rate constant which characterizes ET can be described by both a low frequency medium vibrational mode and a high frequency intramolecular vibrational mode.

At a high temperature regime the constant  $k_{ij}(s \rightarrow 0^+)$  is in the form [21]:

$$\begin{aligned} k_{ij} = & \int_0^\infty W_{ij}(t)dt = \frac{2\pi}{\hbar} V_{ij}^2 \left(\frac{1}{4\pi\lambda_{mij}k_B T}\right)^{1/2} \exp(-S_{cij}) \\ & \times \sum_{n=0}^\infty \frac{S_{cij}^n}{n!} \exp\left[-\frac{(G_{ji} + \lambda_{mij} + n\hbar\omega_{cij})^2}{4\lambda_{mij}k_B T}\right]. \end{aligned} \quad (16)$$

Here,  $G_{ij} = \epsilon_i - \epsilon_j$  and  $S_{cij} = \frac{1}{2\hbar} m_{cij} \omega_{cij} (d_{ci} - d_{cj})^2$  is the scaled reorganization constant for the high frequency  $ij$ -th mode, which is nonzero when electron is transferring from the state  $|i\rangle$  to the state  $|j\rangle$ , and  $\lambda_{mij} = \frac{1}{2} m_{mij} \omega_{mij}^2 (d_{mi} - d_{mj})^2$  is the reorganization energy of the low-frequency mode when the electron is transferring from the state  $|i\rangle$  to the state  $|j\rangle$ . The back electron transfer reaction rate constant can be calculated by using the detailed balance relation and can be expressed in the form  $k_{ji} = k_{ij} \exp(-G_{ij}/k_B T)$ .

The quantum yields  $\Phi_L$ ,  $\Phi_M$  of electronic escape via branch  $L$ ,  $M$  and the quantum yields  $\Phi_G$  of direct ground state recombination can be characterized for 5-sites sequential kinetic



model by the expressions

$$\phi_G = \frac{2\Gamma_1}{\hbar} P_1(s \rightarrow 0^+), \quad (17a)$$

$$\phi_L = \frac{2\Gamma_L}{\hbar} P_5(s \rightarrow 0^+), \quad (17b)$$

$$\phi_M = \frac{2\Gamma_M}{\hbar} P_4(s \rightarrow 0^+), \quad (17c)$$

where the expression  $\Phi_L + \Phi_M + \Phi_G = 1$  have to be fulfilled. The analytical expressions for the ratio of the quantum yields have the forms

$$\frac{\phi_L}{\phi_M} = \frac{k_{13}k_{35}(\frac{2\Gamma_M}{\hbar}k_{24} + k_{21}(k_{42} + \frac{2\Gamma_M}{\hbar}))\frac{2\Gamma_L}{\hbar}}{k_{12}k_{24}(\frac{2\Gamma_L}{\hbar}k_{35} + k_{31}(k_{53} + \frac{2\Gamma_L}{\hbar}))\frac{2\Gamma_M}{\hbar}}, \quad (18a)$$

$$\frac{\phi_L}{\phi_G} = \frac{k_{13}k_{35}\frac{2\Gamma_L}{\hbar}}{(\frac{2\Gamma_L}{\hbar}k_{35} + k_{31}(k_{53} + \frac{2\Gamma_L}{\hbar}))\frac{2\Gamma_1}{\hbar}}. \quad (18b)$$

The results of numerical calculations of QY's rate constants for the sequential model in both branches of RC for different samples of RC are collected in Table I.

The expressions for the electron transfer are given by the inverse Laplace transformation. Therefore firstly we apply the Laplace transformation to  $P(t)$  in system of Eqs. 16. Where the Laplace transformation is defined as

$$P(s) = \int_0^\infty e^{-st} P(t) dt. \quad (19)$$

Next we apply the inverse Laplace transformation of  $P(s)$  where the inverse Laplace transformation is represented by a set of simple poles of  $P(s)$ . Evaluating it we obtain

$$P(t) = \sum_{j=1}^5 a_j e^{k_j t}, \quad (20)$$

where  $a_j$  are amplitudes and  $k_j$  are rate kinetic constants describing the electron transfer.

With using the model described above we would like to find kinetic of the reaction centers of *Chloroflexus aurantiacus* [17] where on the  $M$ -branch the BChl $_M$  is replaced by BPh $_M$  in corresponding position. Thus *C. aurantiacus* RCs contain altogether three BPh molecules and only one BChl monomer. To characterized *C. aurantiacus* we start from the set of parameters that characterize the kinetics of wild-type (WT) RCs of Rb.sphaeroides. We use the following values of input parameters: reorganization energies  $\lambda_{ij} = 800 \text{ cm}^{-1}$ , electronic couplings  $S_{ij} = 0.5 \text{ cm}^{-1}$ , high frequency modes  $\omega_{ij} = 1500 \text{ cm}^{-1}$  where  $i, j = 1, 3, 5$

for  $L$ -side and  $i, j = 1, 2, 4$  for  $M$ -side of RC. The values for electronic couplings  $V_{24} = V_{35} = 32 \text{ cm}^{-1}, V_{12} = V_{13} = 20 \text{ cm}^{-1}$  were used. The sink parameters  $2\Gamma_M/\hbar = 2\Gamma_L/\hbar = (200\text{ps})^{-1}, 2\Gamma_1/\hbar = (170\text{ps})^{-1}$  were used in accordance with experimental observation which characterize the ET to quinone molecules and decay to the ground state. Because of  $\text{BChl}_M$  is replaced by  $\text{BPh}_M$  in corresponding position we decrease the free energy in site 2. The calculated rate constants and quantum yields for the concrete energy levels are collected in Table I. We get the following occupation probabilities for different sites:

$$\begin{aligned}
P_1(t) &= 0.05e^{-0.6t} + 0.15e^{-0.37t} + 0.8e^{-0.22t}, \\
P_2(t) &= -0.25e^{-0.6t} + 0.05e^{-0.37t} + 0.2e^{-0.22t}, \\
P_3(t) &= -0.03e^{-0.6t} - 0.96e^{-0.37t} + 0.99e^{-0.22t}, \\
P_4(t) &= 0.2e^{-0.6t} - 0.07e^{-0.37t} - 0.44e^{-0.22t} + 0.3e^{-0.01t} + 0.01e^{-0.009t}, \\
P_5(t) &= 0.02e^{-0.6t} + 0.8e^{-0.37t} - 1.52e^{-0.22t} - 0.4e^{-0.01t} + 1.1e^{-0.009t}. \quad (21a)
\end{aligned}$$

The exponential components with very small amplitudes were neglected in the expressions above. Time evolution of the occupation probabilities is shown in the Fig.2.

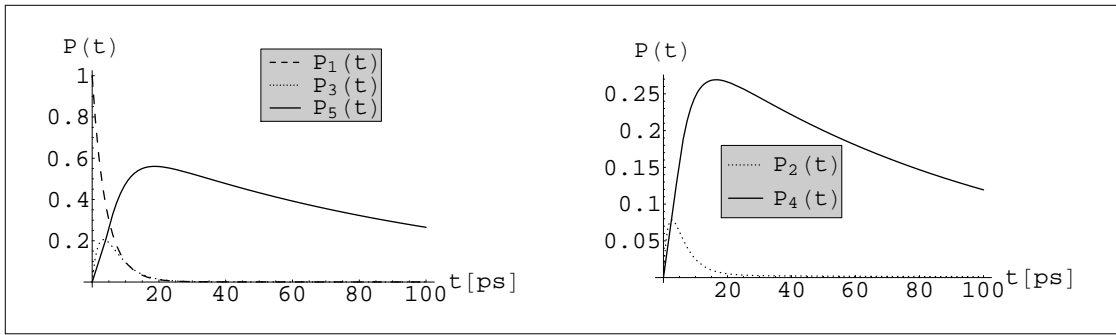


FIG. 2: The occupation probabilities  $P(t)$  for the reaction center *Chloroflexus aurantiacus* in the case if  $V_{12} = V_{13}$ .

We can see that in this case we get electron transfer through the M branch, which is not in accordance with experimental observation. To avoid this discrepancy we must assume the asymmetry in the electronic coupling. To describe experimental kinetic of *Chloroflexus aurantiacus* RC we used the following asymmetry in electronic couplings:  $V_{12} = 10 \text{ cm}^{-1}$  and  $V_{13} = 15 \text{ cm}^{-1}$ . We weakly decrease the coupling constants in comparison with previous case, because of the kinetic in this RC is slower then in the WT RC. The calculated rate

constants and quantum yields for the concrete energy levels are shown in Table I, second line. We found

$$\begin{aligned}
P_1(t) &= 0.002e^{-0.53t} + 0.018e^{-0.34t} + 0.98e^{-0.12t}, \\
P_2(t) &= -0.05e^{-0.53t} + 0.005e^{-0.34t} + 0.04e^{-0.12t} + 0.005e^{-0.01t}, \\
P_3(t) &= -0.4e^{-0.34t} + 0.4e^{-0.12t}, \\
P_4(t) &= 0.053e^{-0.53t} - 0.003e^{-0.34t} - 0.22e^{-0.12t} + 0.13e^{-0.01t} + 0.04e^{-0.009t}, \\
P_5(t) &= 0.4e^{-0.34t} - 1.3e^{-0.12t} - 0.5e^{-0.01t} + 1.4e^{-0.009t}.
\end{aligned} \tag{22a}$$

In Figure 3 the behavior of the occupation probabilities  $P_i(t)$  is shown.

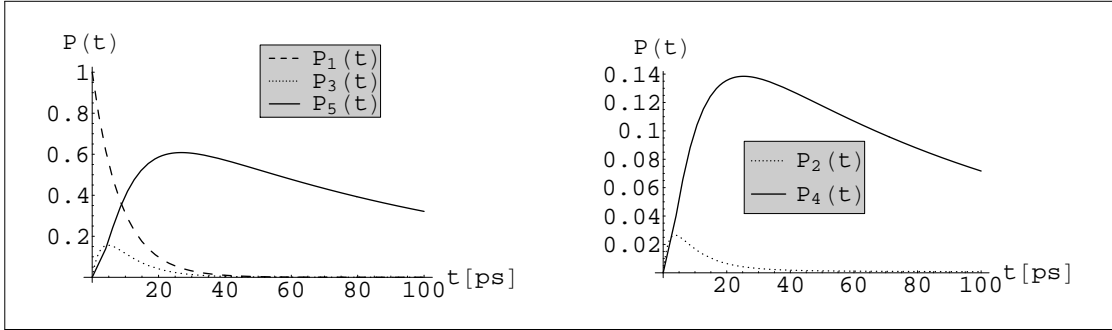


FIG. 3: The occupation probabilities  $P(t)$  for the reaction center *Chloroflexus aurantiacus* in the case if  $V_{12} \neq V_{13}$ .

Now we want to elucidate the electron transfer in  $H(M182)L$ . In this mutant  $BChl_M$  is replaced with  $BPh_M$ . The new cofactor is referred to as  $\phi_M$ . It is reasonable that in the  $H(M182)L$  mutant the state  $P^+\phi_M^-$  is lower in energy than  $P^+BChl_M^-$  in WT [22]. To explain the electron transfer in this mutant we started from incoherent model. In this model we assume that the energy of  $P^+\phi_M^-$  is lower than the free energy of the state  $P^+BPh_M^-$  [23]. The value of the free energies used to calculate the rate constant are listed in Table I.

The occupation probabilities  $P_i(t)$  in the case of  $H(M182)L$  mutant are found in the form

$$\begin{aligned}
P_1(t) &= 0.33e^{-0.38t} + 0.67e^{-0.25t}, \\
P_2(t) &= -0.02e^{-0.52t} - 0.07e^{-0.38t} - 0.23e^{-0.25t} + 0.32e^{-0.0006t}, \\
P_3(t) &= -1.4e^{-0.38t} + 1.4e^{-0.25t}, \\
P_4(t) &= 0.04e^{-0.52t} - 0.036e^{-0.38t} - 0.04e^{-0.25t} + 0.036e^{-0.0006t}, \\
P_5(t) &= 1.1e^{-0.38t} - 1.602e^{-0.25t} + 0.5e^{-0.01t} + 0.002e^{-0.0006t},
\end{aligned} \tag{23a}$$

and the behavior of the occupation probabilities is shown in Fig.4. It was assume that the

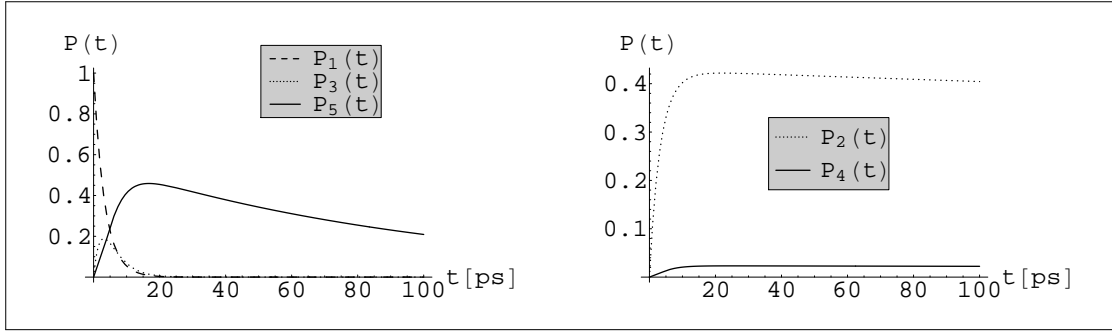


FIG. 4: The occupation probabilities  $P_i(t)$  for the mutant  $H(M182)L$  in the case of incoherent model of electron transfer.

free energy of  $P^+\phi_M^-$  is significantly below  $P^+BPh_M^-$  because of the electron transfer stops at  $\phi_M$ . We get a very small probability to find electron on  $BPh_M$  but the quantum yields through the branch  $M$  is substantial(Table I).

Now we intend to elucidate the observed ET kinetics with partially coherent models. It means, that we assume that the reorganization energy for ET from state  $P^+\phi_M^-$  to state  $P^+BPh_M^-$  is practically zero. The electron kinetic have to be described by the following

system of equations

$$\begin{aligned} \partial_t P_1(t) = & -\left(\frac{2\Gamma_1}{\hbar} + k_{12} + k_{13}\right)P_1(t) \\ & + k_{21}P_2(t) + k_{31}P_3(t), \end{aligned} \quad (24a)$$

$$\partial_t P_2(t) = -k_{21}P_2(t) - \int_0^t W_{24}(t-\tau)P_2(\tau)d\tau + k_{12}P_1(t) + \int_0^t W_{42}(t-\tau)P_4(\tau)d\tau \quad (24b)$$

$$\partial_t P_3(t) = -(k_{35} + k_{31})P_3(t) + k_{13}P_1(t) + k_{53}P_5(t), \quad (24c)$$

$$\partial_t P_4(t) = -\frac{2\Gamma_M}{\hbar}P_4(t) - \int_0^t W_{42}(t-\tau)P_4(\tau)d\tau + \int_0^t W_{24}(t-\tau)P_2(\tau)d\tau, \quad (24d)$$

$$\partial_t P_5(t) = -\left(\frac{2\Gamma_L}{\hbar} + k_{53}\right)P_5(t) + k_{35}P_3(t). \quad (24e)$$

In this case the memory function  $W_{24} = W_{42}$  can be expressed in the form:  $W_{24}(t) = 2\pi \frac{|V_{24}|^2}{\hbar^2} \text{Re} \left\{ \exp \left[ -\frac{\Gamma_M + \Gamma_2}{\hbar} t \right] \exp \left[ \frac{i(\varepsilon_2 - \varepsilon_4)}{\hbar} t \right] \right\}$ , where  $\Gamma_2 = 0$  for our kinetic model. We now use this partially coherent model of RC to describe  $H(M182)L$  mutation of RC. The results of our numerical computations are collected in Table I. We found the following expressions for occupation probabilities  $P_i(t)$ :

$$\begin{aligned} P_1(t) &= 0.6e^{-0.42t} + 0.38e^{-0.3t} + 0.02e^{-0.002t}, \\ P_2(t) &= -0.3e^{-0.42t} - 0.201e^{-0.3t} + 0.001e^{-0.009t} + 0.5e^{-0.002t} + 0.0004e^{-0.005t} \sin(31t), \\ P_3(t) &= -1.4e^{-0.42t} + 1.4e^{-0.3t}, \\ P_4(t) &= -0.03e^{-0.42t} - 0.02e^{-0.3t} + 0.03e^{-0.009t} + 0.02e^{-0.002t} - 0.0006e^{-0.005t} \sin(31t), \\ P_5(t) &= e^{-0.42t} - 1.41e^{-0.3t} + 0.3e^{-0.01t} + 0.01e^{-0.009t} + 0.1e^{-0.002t}. \end{aligned} \quad (25a)$$

The behavior of the occupation probabilities  $P_i(t)$  is shown in Fig.5. The calculated values of parameters for coherent model which describe the mutant  $H(M182)L$  RC's are collected in Table I.

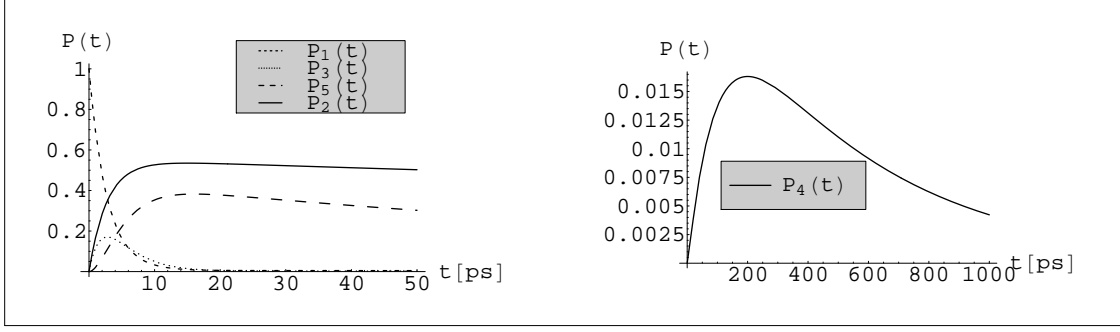


FIG. 5: The occupation probabilities  $P(t)$  for the mutant  $H(M182)L$  in the case of coherent model of electron transfer.

	$T$	$\epsilon_2$	$\epsilon_3$	$\epsilon_4$	$\epsilon_5$	$1/k_{12}$	$1/k_{21}$	$1/k_{13}$	$1/k_{31}$	$1/k_{24}$	$1/k_{42}$	$\Phi_G$	$\Phi_M$	$\Phi_L$
<i>Sample</i>	<i>K</i>	<i>cm<sup>-1</sup></i>	<i>cm<sup>-1</sup></i>	<i>cm<sup>-1</sup></i>	<i>cm<sup>-1</sup></i>	<i>ps</i>	<i>ps</i>	<i>ps</i>	<i>ps</i>	<i>ps</i>	<i>ps</i>			
<i>C.aurant.</i>	295	-50	-450	-1000	-2000	12	15	6	52	2	188	0.02	0.31	0.67
$V_{12} = V_{13}$	200					15	21	5	138	2	1559	0.02	0.25	0.73
<i>C.aurant.</i>	295	-50	-450	-1000	-2000	47	60	11	93	2	188	0.05	0.16	0.79
$V_{12} \neq V_{13}$	200					58	84	10	246	2	1559	0.05	0.12	0.83
<i>H(M182)L</i>	295	-1600	-450	-1000	-2000	8	10005	6	52	37	2.1	0.02	0.41	0.57
<i>Incoherent</i>	200					9	443897	5	138	132	1.8	0.02	0.37	0.61
<i>H(M182)L</i>	295	-850	-450	-1000	-2000	5	292	6	52	4394	4394	0.03	0.12	0.85
<i>Coherent</i>	200					4	1867	5	138	4394	4394	0.02	0.38	0.6

TABLE I: The computed rate constant  $1/k_{ij}$  and quantum yields dependent on temperature for reaction centers and some mutants of RC's. The rate constants  $1/k_{35} = 3(4)ps$  for  $T = 295(200)K$  and  $1/k_{53} = 5166(264544)ps$  for  $T = 295(200)K$  are the same for all RC's and mutations describing in the Table I.

#### IV. CONCLUSION

We have dealing with electron transfer in the reaction center of *Chloroflexus aurantiacus* and *Rhodobacter sphaeroides H(M182)L* mutated RC. In spite of their structural similarity, the functionality is very different. *H(M182)L* mutant reveal the M brunch active in electron transfer. In the previous papers [24, 25, 26, 27, 28] were discussions about what is dominant

factor which causes the asymmetry in the electron transfer. At the beginning it was assumed that the asymmetry in the coupling parameters is dominant. The later the experimental work brought a doubt about dominance of electron coupling as a mechanisms which cause the asymmetry in ET trough branches [22, 23]. Now, it is assume that the asymmetry in energetics also contribute to asymmetry of ET through M and L branches. We have showed that in the *Chloroflexus aurantiacus* RC we must have minimally 2:3 ratio of the electron transfer integrals for  $P^*\phi_M \leftrightarrow P^+\phi_M^-$  and for  $P^*BChl_L \leftrightarrow P^+BChl_L^-$  to explain the observed ET kinetics. In the case of *Rhodobacter sphaeroides H(M182)L* mutated RC we used two models to describe the ET. In incoherent model we must use a very low free energy of the  $P^+\phi_M^-$  state in comparison to the free energy of  $P^+BPh_M^-$  state to get a small probability to find electron on the  $BPh_M$  molecule. Despite this assumption we get relatively strong outlet through the M branch. In the partially coherent model we assume that the ET between molecules  $\phi_M$  and  $BPh_M$  have coherent character, this means that ET is so fast that the bath does not have sufficient time to relax to the new thermal equilibrium before the particle moves away. The result is outlet trough the M branch which is in accordance with experimental observations. The problem of both coherent and incoherent models is that predict not enough decay to the basic state. The similar model ought to be used to characterized electron transfer in PSII (PSI) system, where dimer molecules of  $BChl$  are not so close as in the bacterial reaction centers. The temperature dependence of the kinetics and QYs was also computed. We can see that there are differences in dependence of QY on the temperature in both models which were assumed.

The work was supported in part by VEGA grant 2/7056/27. of the Slovak Academy of Sciences, by the Science and Technology Assistance Agency under contract No. APVT-51-027904.

- 
- [1] J. Deisenhofer *et al.*, Nature **318** (1985) 618.
  - [2] J.P. Allen and J.C. Willams, FEBS Lett. **438** (1998) 5.
  - [3] J. Amesz, J. Photochem. Photobiol. **30** (1995) 89.
  - [4] H. Sakurai, N. Kusumoto, and K. Inoue, Photochem. Photobiol. **64** (1996) 5.
  - [5] J.H. Golbeck, Proc. Natl. Acad. Sci. U.S.A. **90** (1993) 1642.

- [6] W.D. Schubert *et al.*, Nat. Struct. Biol. **3** (1996) 965.
- [7] Van Brederode *et al.*, Biochemistry **36** (1997) 6855.
- [8] B. A. Heller, D. Holten, and C. Kirmaier, Science **269** (1995) 940.
- [9] Ch. Kirmaier and D. Holten, Proc. Natl. Acad. Sci. U.S.A. **87** (1990) 3552.
- [10] E. Takahashi and C. A. Wraight, Biochemistry (1992) 855.
- [11] V. A. Shuvalov and L. N. M. Duysens, Proc. Natl. Acad. Sci. U.S.A. **83** (1986) 1690.
- [12] J. N. Gehlen, M. Marchi, and D. Chandler, Science **263** (1994) 499.
- [13] M.G. Müller, G. Drews and A.R. Holzwarth, Chemical Physics Letters, **258** (1996) 194.
- [14] M. Marchi *et al.*, J. Am. Chem. Soc. **115** (1993) 4178.
- [15] S. Tanaka and R. A. Marcus, J. Phys. Chem. B **101** (1997) 5031.
- [16] M. Bixon, J. Jortner, and M. E. Michel-Beyerle, Chem.Phys. **197** (1995) 389.
- [17] M.G. Müller, K. Griebenow and A.R. Holzwarth, Biochimica et Biophysica Acta, **1098** (1991) 1.
- [18] M. Sparpaglione and S. Mukamel, J. Chem. Phys. **88** (1988) 3263.
- [19] R. Zwanzig, Physica **30** (1964) 1109.
- [20] N. Hashitsume, P. Shibata, and M. Shingu, J. Stat. Phys. **17** (1972) 253.
- [21] J. Jortner, J. Chem. Phys. **64** (1976) 4860.
- [22] E.Katilius, T.Turanchik, S.LIn, A.K.W.Taguchi, N.W.Woodbury, J.Phys.Chem. B **103** (1999) 7386.
- [23] Ch. Kirmaier, Ch. He, and D. Holten, Biochemistry **40** (2001) 12132.
- [24] M. Pudlak, R. Pincak, Physical Review E **68** (2003) 061901.
- [25] M.E.Michel-Beyerle, M.Plato, J.Deisenhhofer, H.Michel, M.Bixon and J.Jortner, Biochim.Biophys.Acta **932** (1988)52.
- [26] R. Pincak, M. Pudlak, Physical Review E **64** (2001) 031906.
- [27] M.Plato, K.Möbius, M.E.Michel-Beyerle, M.Bixon and J.Jortner, J.Am.Chem.Soc. **110** (1988) 7279.
- [28] M. Pudlak, R. Pincak, Chemical Physics Letters **342** (2001) 587.